Available online at www.sciencedirect.com
ScienceDirect
Bioorganic & Medicinal Chemistry Letters 17 (2007) 2299–2304
Bioorganic & Medicinal Chemistry Letters

Discovery of novel 2,3-diarylfuro[2,3-*b*]pyridin-4-amines as potent and selective inhibitors of Lck: Synthesis, SAR, and pharmacokinetic properties

Matthew W. Martin,[a,*] John Newcomb,[b] Joseph J. Nunes,[a] Jean E. Bemis,[a] David C. McGowan,[a] Ryan D. White,[a] John L. Buchanan,[a] Erin F. DiMauro,[a] Christina Boucher,[b] Theodore Faust,[b] Faye Hsieh,[d] Xin Huang,[c] Josie H. Lee,[b] Stephen Schneider,[b] Susan M. Turci[b] and Xiaotian Zhu[c]

[a]*Department of Medicinal Chemistry, Amgen Inc., One Kendall Square, Building 1000, Cambridge, MA 02139, USA*
[b]*Department of HTS and Molecular Pharmacology, Amgen Inc., One Kendall Square, Building 1000, Cambridge, MA 02139, USA*
[c]*Department of Molecular Structure, Amgen Inc., One Kendall Square, Building 1000, Cambridge, MA 02139, USA*
[d]*Department of Pharmacokinetics and Drug Metabolism, Amgen Inc., One Amgen Center Drive, Thousand Oaks, CA 91320, USA*

Received 20 November 2006; revised 12 January 2007; accepted 12 January 2007
Available online 24 January 2007

Abstract—2,3-Diarylfuro[2,3-***b***]pyridine-4-amines are a novel class of potent and selective inhibitors of Lck. The discovery, synthesis, and structure activity relationships of this series of inhibitors are reported. The most promising compounds were also profiled to deduce their pharmacokinetic properties.

The lymphocyte-specific kinase (Lck) is a cytoplasmic tyrosine kinase of the Src family expressed in T cells and natural killer cells.[1] Genetic evidence in both mice and humans demonstrates that Lck activity is important for signaling mediated by the T cell receptor (TCR) and leads to normal T cell development and activation.[2] These findings suggest that a small molecule inhibitor of Lck could be a useful immunosuppressive for the treatment of T cell-mediated autoimmune and inflammatory disorders and/or organ transplant rejection.

A number of groups, including our own,[3] have previously reported the synthesis and characterization of Lck kinase inhibitors.[4] Potent and orally bioavailable Lck inhibitors have also been demonstrated to have inhibitory activities in vivo in several models of T cell-dependent immune responses.[3,4d,e]

We recently described the discovery of a novel series of furanopyrimidines, exemplified by 5,6-diphenyl-*N*-(2-(piperazin-1-yl)ethyl)furo-[2,3-*d*]pyrimidin-4-amine (compound **1**, Fig. 1), as potent and selective inhibitors of Lck and T cell proliferation.[5] X-ray crystallization studies of **1** bound to Lck[6] revealed that the pyrimidine core in **1** binds to the linker region through two hydrogen bonds (Fig. 2): methionine 319 donates a backbone NH to the N1 pyrimidine acceptor and the carbonyl from Glu 317 accepts the CH in the 2-position.[7] Interestingly, the N3 of the pyrimidine ring does not appear to be engaged in any H-bond interactions.

Based on this observation, we theorized that removal of the N3 nitrogen should provide compounds (furanopyridines) with similar biological activity, and possibly

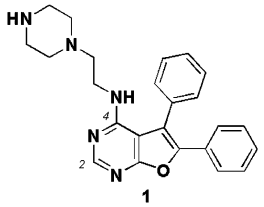

1

Lck IC_{50} = 0.081 μM
KDR IC_{50} = 2.6 μM
Anti-CD3/CD28 IL-2 IC_{50} = 0.71 μM

Figure 1. Structure and activity of furanopyrimidine **1**.

Keywords: Lck inhibitor; Kinase inhibitor.
* Corresponding author. Tel.: +1 617 444 5013; fax: +1 617 621 3908; e-mail: matmarti@amgen.com

0960-894X/$ - see front matter © 2007 Elsevier Ltd. All rights reserved.
doi:10.1016/j.bmcl.2007.01.048

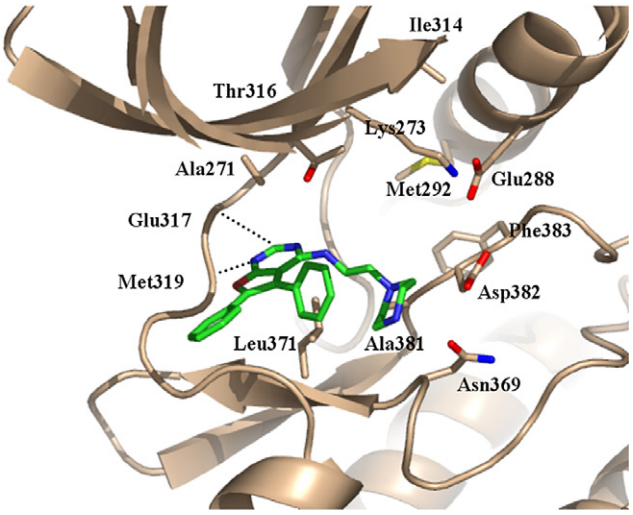

Figure 2. X-ray structure of furanopyrimidine **1** bound to Lck.

improved selectivity. Herein, we describe the synthesis, structure activity relationships, and pharmacokinetic properties of a series of substituted 2,3-diarylfuro[2,3-*b*]pyridin-4-amines, a new class of small molecule inhibitors of Lck.[8]

We developed a concise route for the construction of the desired 2,3-diarylfuro[2,3-*b*]pyridin-4-amines. As illustrated in Scheme 1, the key step was the use of Balme's procedure for the synthesis of furo[2,3-*b*]pyridones.[9] In this reaction, iodopyridone **3** was treated sequentially with phenylacetylene and iodobenzene to afford furanopyridone **4** in good yield via a one-pot coupling–cyclization–deprotection process. Subsequent chlorination with phosphorus oxychloride provided 4-chlorofuranopyridine **5**, which was converted to the 2,3-diarylfuro[2,3-*b*]pyridin-4-amines **6** and **7** via a palladium-catalyzed

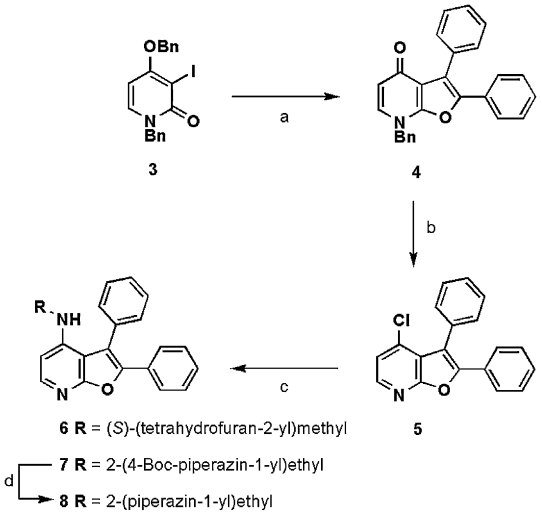

Scheme 1. Synthesis of 2,3-diphenylfuro[2,3-*b*]pyridin-4-amines. Reagents and conditions: (a) phenylacetylene, $PdCl_2(PPh_3)_2$, CuI, Et_3N, CH_3CN, 60 °C, 24 h then PhI, 60 °C, 24 h, 63%; (b) $POCl_3$, 110 °C, 18 h, 57%; (c) RNH_2, $Pd(OAc)_2$, BINAP, K_2CO_3, toluene, 130 °C, 18 h; (d) CF_3CO_2H, CH_2Cl_2, rt, 2.5 h, 68% (two steps).

amination.[10] Compound **7** was then reacted with trifluoroacetic acid to effect *N*-Boc deprotection and afford furanopyridine **8**.

Compounds **6** and **8** were tested for inhibitory activity against Lck in a homogeneous time-resolved fluorescent (HTRF) kinase assay. For the purposes of determining kinase selectivity, the compounds were also screened against the related kinases KDR, Ack1, and JAK3.[11] Cellular activity was measured by testing the compounds for the inhibition of T cell receptor mediated IL-2 production in human T cells as well as for the inhibition of T cell activation in a human mixed lymphocyte reaction.[12]

The initial data for this novel series of inhibitors shown in Table 1. While neither compound exhibited the desired selectivity profile, the nature of the amine in the 4-position proved to be critical. Whereas the 4-(2-piperazin-1-yl)ethylamine derivative **8** exhibited modest potency (0.21 μM), the (*S*)-(tetrahydrofuran-2-yl)methylamine derivative **6** was significantly less potent (2.1 μM). This is in sharp contrast to the related furanopyrimidines, where many more groups were tolerated.[5] To better understand this phenomenon, we obtained a co-crystal structure of furanopyridine **8** with Lck.

As shown in Figure 3,[13] furanopyridine **8** binds to Lck in a manner similar to furanopyrimidine **1**, with the pyridine nitrogen accepting a backbone NH from Met 319 and the carbonyl from Glu 317 accepting the CH in the 6-position of the pyridine ring. The 2-phenyl group points out of the enzyme toward solvent, providing an area to introduce polar solubilizing groups for better cell penetration. Interestingly, both **1** and **8** exhibit potency despite not filling the hydrophobic pocket.[14] In addition, the piperidine ring fills the smaller pocket adjacent to the ribose-binding pocket allowing for a key interaction between the piperidine NH and Asn 369. The inability of furanopyridine **6** to make this interaction (it has no NH to donate) could explain its decreased potency relative to **8**.

With these initial data and structural information in hand, we carried out structure–activity relationship studies designed to identify the substituents for increased potency, selectivity, and optimal pharmacokinetic properties. Our work focused on two areas: substitution on the 2-phenyl ring and optimization of the amine side chain in the 4-position. To construct the desired compounds, we used the synthetic plan outlined in Scheme 2.

The new route was based on a revised version of the chemistry outlined in Scheme 1. Substituting 4-(benzyloxy)phenylacetylene for phenylacetylene in the key coupling–cyclization–deprotection step afforded key intermediate furanopyridone **9**. Palladium-catalyzed hydrogenation and subsequent chlorination with oxalyl chloride afforded 4-chlorofuranopyridine **10**, which contained two handles for examining the desired substitutions. As in the original route, palladium-catalyzed amination introduced the side chain in the

Table 1. Initial furanopyridine SAR (IC_{50}, μM)[a]

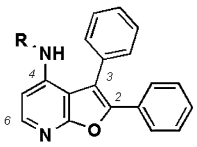

Compound	R	Lck	KDR	Ack1	JAK3	IL-2[b]	huMLR[c]
6	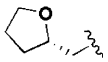	2.1	4.2	0.11	0.026	5.2	4.0
8	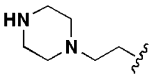	0.21	0.36	0.42	0.14	1.2	0.62

[a] IC_{50} values are means of two or more separate determinations, in duplicate.
[b] IL-2: anti-CD3/CD28-induced T cell IL-2 secretion assay.
[c] huMLR: human Mixed Lymphocyte Reaction.

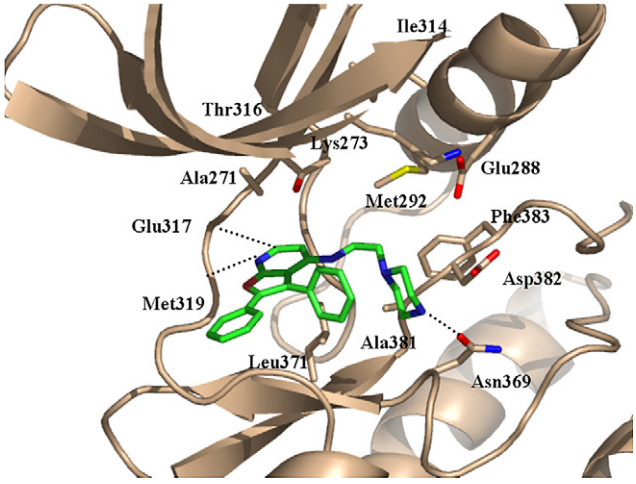

Figure 3. X-ray structure of furanopyridine **8** bound to Lck.

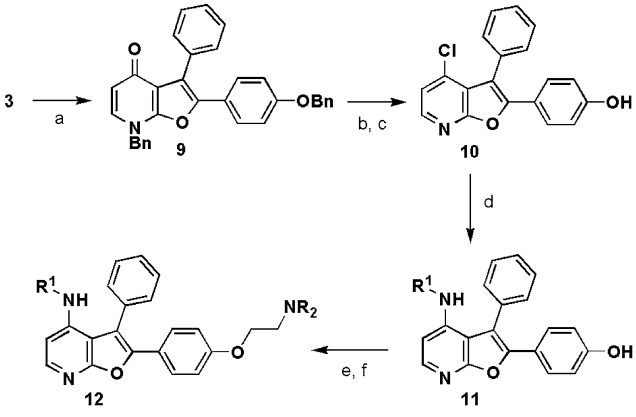

Scheme 2. Modified synthesis of 2,3-diphenylfuro[2,3-*b*]pyridin-4-amines. Reagents and conditions: (a) 4-(benzyloxy)phenylacetylene, $PdCl_2(PPh_3)_2$, CuI, Et_3N, CH_3CN, 60 °C, 24 h then PhI, 60 °C, 24 h, 61–62%; (b) H_2 (g), Pd/C, EtOAc–CH_2Cl_2, rt, 16 h, 71–86%; (c) $(COCl)_2$, cat. DMF, $CHCl_3$, reflux, 2 h, 65%; (d) R^1NH_2, $Pd(OAc)_2$, BINAP, K_2CO_3, toluene, 130 °C, 18 h, 46–60%; (e) $ClCH_2CH_2NR_2$, Cs_2CO_3, DMF, 85 °C, 16 h; (f) CF_3CO_2H, CH_2Cl_2, 0 °C to rt, 2 h, 82–91% (two steps).

4-position (compound **11**). Subsequent alkylation of the phenol and deprotection afforded the desired compounds **12**.

Table 2 summarizes our results for the introduction of solubilizing groups on the 2-phenyl group. In general, the addition of the basic amine side chains increased enzyme potency four- to ten-fold relative to **8**. Selectivity against KDR, Ack1, and JAK3 remained unchanged, ranging from two- to five-fold over Lck. Consistent with what was observed for **8**, all compounds experienced an approximately five- to ten-fold shift (relative to the enzyme IC_{50}) when tested for cell activity in the IL-2 secretion assay. A much smaller shift (~2-fold) was observed when the compounds were tested in the huMLR, with compounds **13**, **15**, **16**, and **17** exhibiting IC_{50} values between 20 and 60 nM.

Having established the benefits of substituting the 2-phenyl ring, we next explored the SAR of the 4-amino side chain. We were interested in cyclic amines that could engage Asn 369 and provide compounds with increased enzyme and cell potency relative to piperidine derivative **17**. As shown in Table 3, replacing the piperazine with aromatic heterocycles led to a decrease in potency in all examples tested. Presumably, none of these compounds can form favorable H-bond interactions with Asn 369.

We also examined the pharmacokinetic properties of a number of cell potent compounds. Compounds **8**, **13**, **15**, **16**, and **17** were tested for microsomal stability and dosed iv in Sprague–Dawley rats (Table 4). Compound **8** (at 0.62 μM, the least potent in cells) showed moderate clearance (1.2 L/h/kg) and a short half-life (1.5 h). In contrast, compounds **13**, **15**, **16**, and **17**, all of which exhibited promising cellular activity, each had undesirable PK properties. All four compounds were cleared at a rate higher than hepatic blood flow (~8–11 L/h/kg) and showed a correspondingly high volume of distribution (7–122 L/kg). Furthermore, in vitro microsomal clearance was not predictive of in vivo stability.[15] Whereas compounds **15** and **16** exhibited

Table 2. SAR: variations on the 6-phenyl group (IC_{50}, μM)[a]

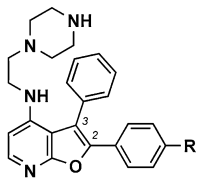

Compound	R	Lck	KDR	Ack1	JAK3	IL-2[b]	huMLR[c]
8	**H**	0.21	0.36	0.42	0.14	1.2	0.62
13	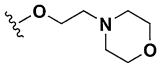	0.022	0.057	0.15	0.032	0.13	0.014
14	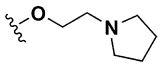	0.054	0.21	0.17	0.11	0.65	0.17
15	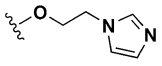	0.030	0.16	0.084	0.025	0.47	0.057
16	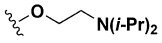	0.019	0.067	0.18	0.044	0.25	0.018
17	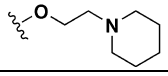	0.029	0.10	0.12	0.071	0.51	0.061

[a] IC_{50} values are means of two or more separate determinations, in duplicate.
[b] IL-2: Anti-CD3/CD28-induced T cell IL-2 secretion assay.
[c] huMLR: human mixed lymphocyte reaction.

Table 3. SAR: variations on the 4-amino side chain (IC_{50}, μM)[a]

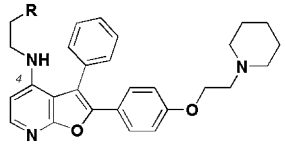

Compound	R	Lck	KDR	Ack1	JAK3
17	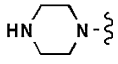	0.029	0.10	0.12	0.071
18		1.6	4.7	0.18	0.080
19		0.17	0.37	0.020	0.037
20	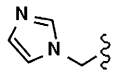	0.38	1.7	0.93	1.4

[a] IC_{50} values are means of two or more separate determinations, in duplicate.

high clearance both in vivo and in vitro, compounds **13** and **17** showed promising in vitro clearance but high rates of in vivo clearance. The observed PK properties are best interpreted in the context of the clog *P* for each of the compounds.[16] With the exception of compound **15**, the clog *P* increased with the introduction of the polar amine side chains, with the high clog *P* values of **16** and **17** accounting for the large clearance values.[17]

Table 4. Pharmacokinetic parameters following iv Dose in Sprague-Dawley Rats[a,b]

Compound	CL (L/h/kg)	V_{ss} (L/kg)	$t_{1/2}$ (h)	CL_{int}[c] (μL/min/mg)	clog *P*[d]
8	1.2	2.3	1.5	137	4.7
13	7.7	4.7	5.3	<5	4.8
15	11.5	7.2	0.8	100	4.4
16	34.1	122	3.1	120	6.6
17	11.3	60	4.7	50	6.0

[a] $n = 3$ animals per study.
[b] Dosed at 1 mg/kg as a solution in DMSO.
[c] In vitro intrinsic clearance after incubation with rat liver microsomes. Compound concentration = 1 μM, microsomal protein = 0.25 mg/mL.
[d] Determined using ACDLabs 8.0.

In summary, we have reported the discovery of a novel class of 2,3-diarylfuro[2,3-*b*]pyridin-4-amines that are potent and selective inhibitors of Lck. These compounds show promising cellular activity when tested in a human MLR and in an anti-CD3/CD28-induced IL-2 secretion assay. Despite non-optimal pharmacokinetic properties, these initial compounds show the potential of furanopyridines as a new class of Lck inhibitors. Future work will aim to improve the potency and pharmacokinetic properties with the hope of identifying compounds suitable for in vivo studies.

Acknowledgments

We are grateful to our colleagues Linda Epstein, Yan Gu, Paul Rose, and Huilin Zhao for Lck protein expres-

sion and purification; Yuping Chen for the microsomal stability data; and Antonio Oliveira-dos-Santos for assistance with the biological assays.

References and notes

1. Marth, J. D.; Lewis, D. B.; Cooke, M. P.; Mellins, E. D.; Gearn, M. E.; Samelson, L. E.; Wilson, C. B.; Miller, A. D.; Perlmutter, R. M. *J. Immunol.* **1989**, *142*, 2430.
2. (a) Goldman, F. D.; Ballas, Z. K.; Schutte, B. C.; Kemp, J.; Hollenback, C.; Noraz, N.; Taylor, N. *J. Clin. Invest.* **1998**, *102*, 421; (b) Molina, T. J.; Kishihara, K.; Siderovskid, D. P.; van Ewijk, W.; Narendran, A.; Timms, E.; Wakeham, A.; Paige, C. J.; Hartmann, K.-U.; Veillette, A.; Davidson, D.; Mak, T. W. *Nature* **1992**, *357*, 161; (c) Straus, D. B.; Weiss, A. *Cell* **1992**, *70*, 585.
3. (a) Martin, M. W.; Newcomb, J.; Nunes, J. J.; McGowan, D. C.; Armistead, D. M.; Boucher, C.; Buchanan, J. L.; Buckner, W.; Chai, L.; Elbaum, D.; Epstein, L. F.; Faust, T.; Flynn, S.; Gallant, P.; Gore, A.; Gu, Y.; Hsieh, F.; Huang, X.; Lee, J. H.; Metz, D.; Middleton, S.; Mohn, D.; Morgenstern, K.; Morrison, M. J.; Novak, P. M.; Oliveira-dos-Santos, A.; Powers, D.; Rose, P.; Schneider, S.; Sell, S.; Tudor, Y.; Turci, S. M.; Welcher, A. A.; White, R. D.; Zack, D.; Zhao, H.; Zhu, L.; Zhu, X.; Ghiron, C.; Amouzegh, P.; Ermann, M.; Jenkins, J.; Johnston, D.; Napier, S.; Power, E. *J. Med. Chem.* **2006**, *49*, 4981; (b) DiMauro, E. F.; Newcomb, J.; Nunes, J. J.; Bemis, J. E.; Boucher, C.; Buchanan, J. L.; Buckner, W. H.; Cee, V. J.; Chai, L.; Deak, H. L.; Epstein, L. F.; Faust, T.; Gallant, P.; Geuns-Meyer, S. D.; Gore, A.; Gu, Y.; Henkle, B.; Hodous, B. L.; Hsieh, F.; Huang, X.; Kim, J. L.; Lee, J. H.; Martin, M. W.; Masse, C. E.; McGowan, D. C.; Metz, D.; Mohn, D.; Morgenstern, K. A.; Oliveira-dos-Santos, A.; Patel, V. F.; Powers, D.; Rose, P. E.; Schneider, S.; Tomlinson, S. A.; Tudor, Y.-Y.; Turci, S. M.; Welcher, A. A.; White, R. D.; Zhao, H.; Zhu, L.; Zhu, X. *J. Med. Chem.* **2006**, *49*, 5671.
4. (a) Trevillyan, J. M.; Chiou, X. G.; Ballaron, S. J.; Tang, Q. M.; Buko, A.; Sheets, M. P.; Smith, M. L.; Putnam, B.; Wiedeman, P.; Tu, N.; Madar, D.; Smith, H. T.; Gubbins, E. J.; Warrior, U. P.; Chen, Y.-W.; Mollison, K. W.; Faltynek, C. R.; Djuric, S. W. *Arch. Biochem. Biophys.* **1999**, *364*, 19; (b) Goldberg, D. R.; Butz, T.; Cardozo, M. G.; Eckner, R. J.; Hammach, A.; Huang, J.; Jakes, S.; Kapadia, S.; Kashem, M.; Lukas, S.; Morwick, T. M.; Panzenbeck, M.; Patel, U.; Pav, S.; Peet, G. W.; Peterson, J. D.; Prokopowicz, A. S.; Snow, R. J.; Sellati, R.; Takahashi, H.; Tan, J.; Tschantz, M. A.; Wang, X.-J.; Wang, Y.; Wolak, J.; Xiong, P.; Moss, N. *J. Med. Chem.* **2003**, *46*, 1337; (c) Das, J.; Moquin, R. V.; Lin, J.; Liu, C.; Doweyko, A. M.; DeFex, H. F.; Fang, Q.; Pang, S.; Pitt, S.; Shen, D. R.; Schieven, G. L.; Barrish, J. C.; Wityak, J. *Bioorg. Med. Chem. Lett.* **2003**, *13*, 2587; (d) Chen, P.; Doweyko, A. M.; Norris, D.; Gu, H. H.; Spergel, S. H.; Das, J.; Moquin, R. V.; Lin, J.; Wityak, J.; Iwanowicz, E. J.; McIntyre, K. W.; Shuster, D. J.; Behnia, K.; Chong, S.; de Fex, H.; Pang, S.; Pitt, S.; Shen, D. R.; Thrall, S.; Stanley, P.; Kocy, O. R.; Witmer, M. R.; Kanner, S. B.; Schieven, G. L.; Barrish, J. C. *J. Med. Chem.* **2004**, *47*, 4517; (e) Borhani, D. W.; Calderwood, D. J.; Friedman, M. M.; Hirst, G. C.; Li, B.; Leung, A. K. W.; McRae, B.; Ratnofsky, S.; Ritter, K.; Waegell, W. *Bioorg. Med. Chem. Lett.* **2004**, *14*, 2613; (f) Burchat, A.; Borhani, D. W.; Calderwood, D. J.; Hirst, G. C.; Li, B.; Stachlewitz, R. F. *Bioorg. Med. Chem. Lett.* **2006**, *16*, 118.
5. DiMauro, E. F.; Newcomb, J.; Nunes, J. J.; Bemis, J. E.; Boucher, C.; Buchanan, J. L.; Buckner, W. H.; Chang, A.; Faust, T.; Hsieh, F.; Huang, X.; Lee, J. H.; Marshall, T. L.; Martin, M. W.; McGowan, D. C.; Schneider, S.; Turci, S. M.; White, R. D.; Zhu, X. *Bioorg. Med. Chem. Lett.* **2007**, *17*. doi:10.1016/j.bmcl.2007.01.057.
6. The kinase domain of human Lck (residues 225–501) with a C-terminal His6 tag was expressed in insect cells and purified by immobilized metal affinity, anion exchange, and size exclusion chromatographies. The protein was then phosphorylated by incubation with 5 mM Mg^{++}· ATP for 10 min at room temperature. Phosphorylated Lck was further purified by anion exchange chromatography and concentrated to 10 mg/mL. The coordinates for the X-ray co-crystal structure of Lck and **1** have been deposited in the PDB. The RCSB ID code is RCSB041056 and the PDB ID code is 2OF4.
7. For a discussion of CH–O hydrogen bonds in protein-ligand complexes, see Pierce, A. C.; Sandretto, K. L.; Bemis, G. W. *Proteins: Struct. Funct. Genet.* **2002**, *49*, 567.
8. Nunes, J. J.; Martin, M. W.; White, R.; McGowan, D.; Bemis, J. E.; Kayser, F.; Fu, J.; Liu, J.; Jiao, X. Y. (Amgen Inc.) Furanopyridine derivatives and methods of use. US Pat. App. 2006046977 A1, **2006**.
9. Bossharth, E.; Desbordes, P.; Monteiro, N.; Balme, G. *Org. Lett.* **2003**, *5*, 2441.
10. For reviews of the Pd-catalyzed amination reaction, see (a) Jiang, L.; Buchwald, S. L. Palladium-catalyzed aromatic carbon–nitrogen bond formation. In *Metal-catalyzed Cross-coupling Reactions*; de Meijere, A., Diederich, F., Eds., 2nd ed.; Wiley-VCH: Weinheim, 2004; p 699; (b) Hartwig, J. F. *Synlett* **2006**, 1283.
11. All kinases were tested at their apparent K_m of ATP with respect to 1 μM of peptide substrate.
12. For descriptions of all assays, see Ref. 3a.
13. The coordinates for the X-ray co-crystal structure of Lck and **8** have been deposited in the PDB. The RCSB ID code is RCSB041054 and the PDB ID code is 2OF2.
14. Previous work has shown that engaging this pocket is a key element necessary for potency. See Ref. 3a.
15. The in vitro intrinsic clearances, CL_{int}, of the test compounds were determined by incubations with rat liver microsomes purchased from BD Biosciences (San Jose, CA). The 400 μL incubations contained 0.25 mg of microsomal protein/mL, 1 mM NADPH, and 2 mM $MgCl_2$ in 50 mM potassium phosphate buffer, pH 7.4. Test compounds were added to the pre-warmed (37 °C) incubation mixtures at the final concentration of 1 μM. At 0, 10, 20, 30, and 40 min following addition of test compound, aliquots of the incubation mixture (35 μL) were collected into an equal volume of acetonitrile + internal standard (1 μM tolbutamide). The samples were centrifuged at 3500*g* for 15 min and analyzed on a liquid chromatography tandem mass spectrometry system consisting of 2 Shimadzu LC-10AD HPLC pumps and a DGU-14A degasser (Shimadzu, Columbia, MD), CTC PAL autoinjector (Leap Technologies, Carrboro, NC) and an API3000 LC-MSMS system. Chromatography was conducted on a Sprite Armor C18 (20 × 2.1 mm, 10μm) analytical column (Analytical Sales and Products, Pompton Plains, NJ) with a 0.5 μm PEEK guard filter, using the following mobile phase gradient program: MPA = H_20 with 0.1% formic acid; MPB = acetonitrile with 0.1% formic acid; 0 min = 98% MPA, 2% MPB; 0.3 min = 98% MPA, 2% MPB; 0.7 min = 5% MPA, 95% MPB; 1.3 min = 5% MPA, 95% MPB; 1.4 min = 98% MPA, 2% MPB; 1.7 min = end of run; approximately 2 min between sample injections. For each compound, peak areas at each time point were converted to the natural log of the %

remaining relative to the 0-min samples. The resulting slope of these values relative to time (k) was converted to in vitro $T_{1/2}$ where $T_{1/2} = -0.693/k$. CL_{int} was calculated using the following relationship: $CL_{int} = (0.693/T_{1/2}) \times (1/0.25\ mg/mL)$.

16. For a discussion of the relationship between calculated and physical properties with successful drug development, see (a) Lipinski, C. A.; Lombardo, F.; Dominy, B. W.; Feeney, P. J. *Adv. Drug Deliv. Rev.* **1997**, *23*, 3; (b) Lipinski, C. A. J. *Pharmacol. Toxicol. Methods* **2000**, *44*, 235.
17. We believe the outlying value for the clog*P* of **15** can be best rationalized by taking into account that these are *calculated* and not measured values for log*P*.